Optimisation of the Hydrodynamic Performance of a wave energy converter in an Integrated Cylindrical WEC-Type Breakwater System

Haoyu Ding
Affiliation: Department of Architecture & Civil Engineering, University of Bath, UK
Full Mailing Address: University of Bath, Claverton Down, Bath, UK, BA2 7AY.
e-mail: hd484@bath.ac.uk

Jun Zang
Affiliation: Department of Architecture & Civil Engineering, University of Bath, UK
Full Mailing Address: University of Bath, Claverton Down, Bath, UK, BA2 7AY.
e-mail: jz235@bath.ac.uk

Peng Jin
Affiliation: School of Marine Science and Engineering, South China University of Technology, China
Full Mailing Address: South China University of Technology, Guangzhou, 510641, China.
e-mail: jinpeng@scut.edu.cn

Dezhi Ning
Affiliation: State Key Laboratory of Coastal and Offshore Engineering, Dalian University of Technology, China
Full Mailing Address: No.2 Linggong Road, Ganjingzi District, Dalian, Liaoning, China, 116024.
e-mail: dzning@dlut.edu.cn

Xuanlie Zhao
Affiliation: College of Shipbuilding Engineering, Harbin Engineering University, China
Full Mailing Address: Harbin Engineering University, Nangang, Harbin, Heilongjiang, Chian, 150009.
e-mail: xlzhao@hrbeu.edu.cn

Yingyi Liu
Affiliation: Research Institute for Applied Mechanics, Kyushu University, Japan
Full Mailing Address: Kyushu University, 744 Motooka, Nishi-ku, Fukuoka, Japan, 819-0395.
e-mail: liuyingyi@riam.kyushu-u.ac.jp

Chris Blenkinsopp
Affiliation: Department of Architecture & Civil Engineering, University of Bath, UK
Full Mailing Address: University of Bath, Claverton Down, Bath, UK, BA2 7AY.
e-mail: cb761@bath.ac.uk

Qiang Chen
Affiliation: International Hurricane Research Center, Florida International University, USA
Full Mailing Address: International Hurricane Research Center, Florida International University, Miami, FL, USA.
e-mail: qchen@fiu.edu

ABSTRACT

Wave energy converters (WECs) are built to extract wave energy. However, this kind of device is still expensive for commercial utilisation. To cut down the cost of WECs by sharing the construction cost with breakwaters, an integrated cylindrical WEC-type breakwater system that includes a cylindrical WEC array in front of a very long breakwater is proposed to extract wave energy and attenuate incident waves. This paper aims to optimise the performance of the integrated cylindrical WEC-type breakwater system. A computational fluid dynamics tool, OpenFOAM®, and a potential flow theory-based solver, HAMS®, are utilised. OpenFOAM® provides viscosity corrections to a modified version of HAMS® in order to accurately and efficiently predict the integrated system's performance. Parametric studies are conducted to optimise the integrated system, and a novel setup with an extra arc structure is found to significantly improve the performance of the integrated system.

1. Introduction

Wave power is reliable, affordable and sustainable form of energy [1]. To extract wave energy, wave energy converters (WECs) are installed in coastal or offshore areas. However, current WEC technology is still unavailable for practical large-scale utilisation, and high cost is a major barrier to widespread use [2]. One possible solution to develop WECs into an affordable commercial technology is to share the construction cost of WECs with other functional structures [3].

Breakwaters are coastal structures designed to provide coastal protection by attenuating incident wave power. This type of structure is appropriate for integration with WECs because both breakwaters and WECs are installed in coastal and nearshore areas. WECs aim to convert wave energy to other functional energy, which can also help breakwaters to attenuate incident wave power. Thus, the integrated WEC-type breakwater system was proposed to share the construction cost and space.

Zhao et al. [4] originally proposed an integrated cylindrical WEC-type breakwater system (hereafter WEC-B system) which comprises heaving oscillating cylindrical WECs attached to the wave-exposed side of a truncated breakwater as shown in Fig. 1. These WECs are connected to a PTO system and restrained by vertical rods. The PTO system then transfers the heave motion of buoys to energy. As for the truncated breakwater, the incident waves are dissipated and reflected as they propagate past the surface-piercing skirt, reducing the wave energy which reaches the coast. An additional advantage is that the component of wave energy reflected from the breakwater can be utilised by the cylindrical WEC array to generate more power (the magnitude of wave energy conversion efficiency, capture width ratio, was raised from 20% without breakwater to 70% with a breakwater in [4]). [5] argued that the heaving oscillating WEC has the potential for highly efficient wave-power conversion in terms of output per unit volume. Considering this advantage, it is valuable to develop this WEC-B system further. The design parameters, including the WEC draft, the gap width between the WEC and the breakwater and dampings, were discussed in [4] to optimise the WEC-B system.

This paper utilises open-source CFD and potential flow solvers to investigate the influence of the ratio of radius to draft of a cylindrical WEC and optimise the system in terms of capture width ratio. In addition, a novel setup of the cylindrical WEC installed with an extra arc structure is proposed and evaluated.

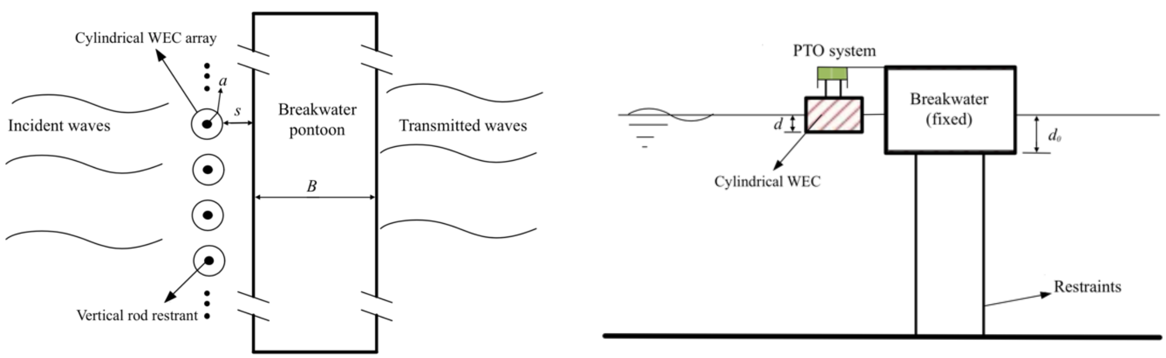

(**a**) (**b**)

Fig. 1 (**a**) the top view and (**b**) the side view of the integrated cylindrical WEC-type breakwater system.

2. Response and capture width ratio

Potential flow theory, which ignores viscous effects, is an efficient method for undertaking parametric research with large numbers of test cases. However, this method will overestimate the motion response and the power conversion efficiency of a heaving oscillating WEC because of the lack of viscous effects [6]. To improve this issue, a viscous computational fluid dynamics (CFD) model is utilised in parallel to provide viscosity corrections to the potential flow theory. Through this approach, the investigation using the modified potential flow theory saves substantial computational time compared with using the CFD tool alone while still providing reasonably accurate results. Thus, the modified potential flow theory is employed in the parametric study of the WEC-B system to optimise this integrated system. In this paper, OpenFOAM® [7] is selected as the CFD tool, and HAMS® [8-10] (https://github.com/YingyiLiu/HAMS) is employed to solve the potential flow theory.

In our computations, the heave response of the heaving oscillating cylindrical WEC buoy is required for calculating the capture width ratio (CWR), which is used to evaluate the efficiency of wave energy extraction. The heave motion can be yielded from the following equation:

$$(-\omega^2(M+\mu_0)-i\omega(\lambda+\lambda_{PTO})+K)\zeta = F_{EX} \quad (1)$$

where M is mass, μ_0 denotes added mass, λ and λ_{PTO} are the viscous damping and damping of the PTO system, respectively, K is the buoyancy stiffness, ζ refers to the motion of the structure and F_{EX} denotes the wave excitation force. F_{EX} is obtained from HAMS® by solving potential flow theories. μ_0 and λ, are both influenced by viscosity. To better represent the viscosity effects, [4] and [11] use the free decay test implemented by physic experiments to calculate μ_0 and λ and substitute them to Eq. 1 to yield the motion of structures. In this paper, the free decay test is simulated by OpenFOAM®. The dynamic viscosity μ_0 is calculated from the free decay period, $T_0 = 2\pi\sqrt{(M+\mu_0)/K}$. Thus,

$$\mu_0 = \frac{{T_0}^2K}{2\pi} - M \quad (2)$$

As for λ, it can be calculated as:

$$\lambda = \frac{2\kappa K}{\omega_0} \quad (3)$$

where $\omega_0 = 2\pi/T_0$, $\kappa = \frac{1}{2\pi}\ln\left(\frac{z_i - z_{i-1}}{z_{i-2} - z_{i-3}}\right)$ and z_i are the successive peak or trough values of the heave response in the free decay test [11]. In this way, ζ can be obtained from Eq. 1 using the viscosity corrections. Because the power generated by the motion of WEC can be denoted as

$$P_{capture} = \frac{1}{2}\lambda_{PTO}\omega^2|\zeta|^2 \quad (4)$$

The optimal damping of the PTO system λ_{PTO} can be defined as:

$$\lambda_{PTO} = \sqrt{\left(K/\omega - \omega(M + \mu_0)\right)^2 + \lambda^2} \quad (5)$$

The CWR is calculated as the ratio of the generated power by the motion of WEC to the incident wave power:

$$\text{CWR} = P_{capture}/P_{incident} \quad (6)$$

where $P_{incident}$ is the incident wave power, it can be calculated as:

$$P_{incident} = \frac{1}{16}\frac{\rho g H^2 \omega D}{k}\left(1 + \frac{2hk}{\sinh 2hk}\right) \quad (7)$$

where H is incident wave height, D is the diameter of the cylindrical WEC, k is wave number and h is water depth [12].

3. Validation

Fig. 2 shows the dimension of the WEC-B system for the validation cases setup based on the experiments detailed in [4]. One heaving oscillating cylindrical WEC with radius (*a*) of 0.135 m and draft (*d*) of 0.2 m is installed in front of a fixed truncated breakwater with a draft of 0.25 m and structure breadth of 0.6 m. The gap width between the cylindrical WEC and the breakwater (*s*) is 0.1 m, the water depth (*h*) is 1 m, and the incident waves are regular waves with a wave height that is kept at a constant value of 0.12 m.

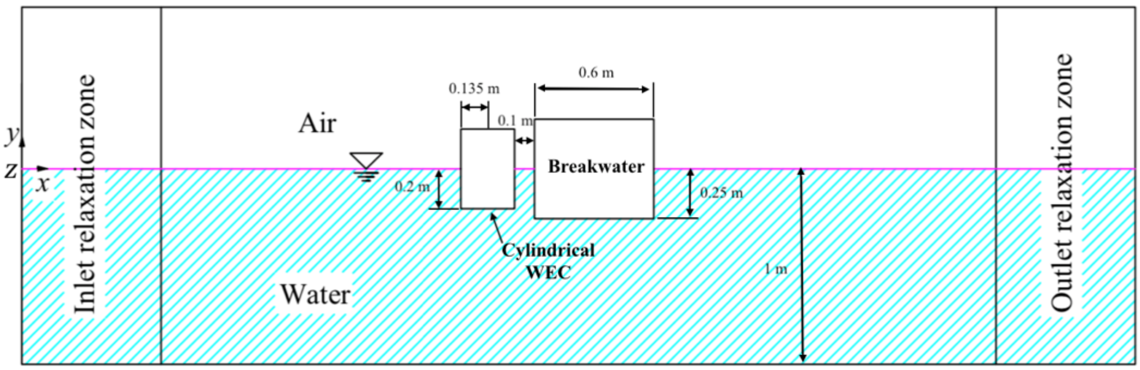

Fig. 2 Schematic of the WEC-B system for validation cases (Side view).

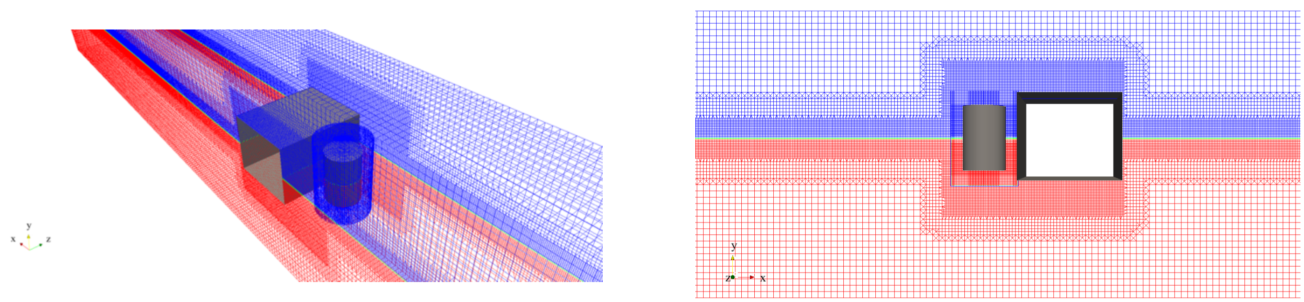

(**a**) (**b**)

Fig. 3 (**a**) The 3D numerical wave tank for validation cases in OpenFOAM®; (**b**) the mesh setup in one cross-section of the numerical wave tank.

Fig. 3 shows the 3D numerical wave tank for the validation cases in OpenFOAM®. The breadth of the numerical wave tank in the *z*-direction is 0.73 m, which is the distance between adjacent cylinders in the original conceptual design. The water depth and the height of the air phase in the *y*-direction are 1 m and 0.8 m, respectively. Based on the discussion about mesh size in a 3D numerical wave tank in [13] and floating structure in [14], a refined mesh is used around the free surface along the *x*- and *z*-axes with a cell size of *l*/200 (*l* is the incident wavelength). The refined mesh size around the structures along the *x*-axis has a cell size of 0.01 m, and $A/8$ in the *y*-direction (A is the incident wave amplitude).

A series of validation cases were implemented using the above numerical model setup. Fig. 4(a) shows comparisons of the heave response amplitude operator (HRAO = heave response/incident wave amplitude) as a function of dimensionless wavenumber, kh, between the original HAMS® results without viscosity and the modified HAMS® results using the method of viscosity corrections in Section 2. The HRAO is much smaller when the viscosity corrections are applied, especially around the natural frequency of the cylindrical WEC (around $kh = 3$). Fig. 4(b) validates HRAO calculated by the potential flow solver with viscosity corrections by comparing them with results from the CFD method and experimental data from [4]. In the lower frequency region ($kh < 2.5$), both HAMS® and OpenFOAM® results agree with experimental data. In the higher frequency region ($kh > 2.5$), the OpenFOAM® results still predict the HRAO accurately compared with experimental results. However, the results of HAMS® are higher than those of both OpenFOAM® and experiments. The overestimation of HRAO using HAMS® may be influenced by the nonlinear wave conditions in the narrow gap between the cylindrical WEC and the breakwater. Nonetheless, the modified HAMS® with viscosity corrections can still predict the general behaviour of the HRAO curve, and the values are generally close to the OpenFOAM® and experimental results.

The transmission coefficient (K_T = transmitted wave height/incident wave height, where the transmitted wave height is obtained from the wave gauge at the central line of the WEC-B system and 1.5 m away from the backside of the breakwater) is shown in

Fig. 5 as a function of wavenumber. Fig. 5 shows good agreement between the results of HAMS®, OpenFOAM® and the experiments described in [4]. In conclusion, the modified HAMS® can is capable of predicting CWR and K_T under various conditions for a parametric study.

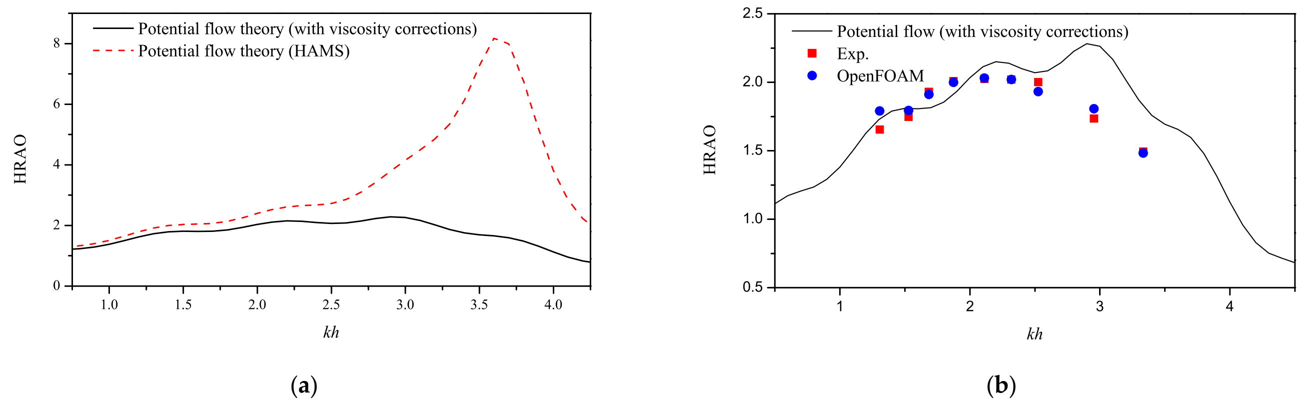

Fig. 4 HRAO of the cylindrical WEC as a function of *kh* with (**a**) the comparison of the original HAMS® and the modified HAMS® with viscosity corrections; (**b**) the comparison of the numerical and experimental results.

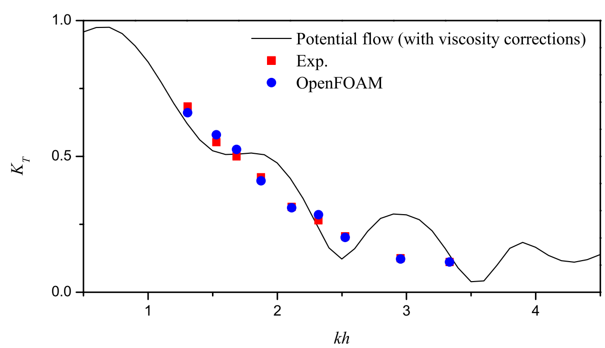

Fig. 5 Comparison of experimental and numerical values of wave transmission coefficient (K_T) as a function of *kh*.

4. Optimisation

4.1 Ratio of radius to draft of the cylinder (*a / d*)

The radius is changed relatively when the draft changes to keep the volume and mass of the cylindrical WEC constant. Thus, the ratio of radius to draft of the cylinder, *a/d*, is investigated. Fig. 6 shows the heave response in decay tests of different cylindrical WECs with varying ratios of radius to draft in time histories obtained via OpenFOAM®. Even though the three cylindrical WECs have the same mass, the curves of the heave response of different cylindrical WECs are different due to the viscosity effects. The viscosity corrections are obtained via the decay tests, and the calculated added mass (as shown in Eq. 3) and viscous damping (as shown in Eq. 4) are listed in Table 1.

Table 1 Viscosity corrections for different ratios of radius to draft of the cylinder.

	Draft 0.2 m	Draft 0.23 m	Draft 0.25 m
Radius of the cylinder (m)	0.135	0.125	0.121
Added mass (kg)	5.247	4.567	4.227
Viscous damping (kg/s)	22.50	19.49	18.06

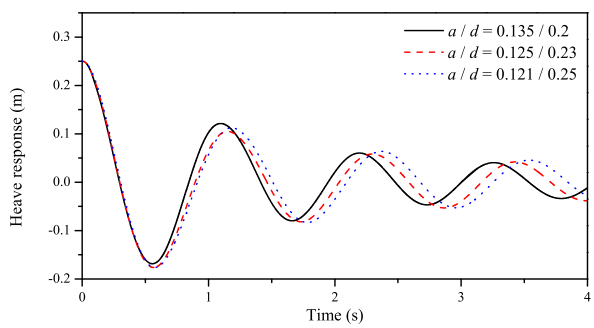

Fig. 6 Decay tests of the cylinders with different ratios of radius to draft.

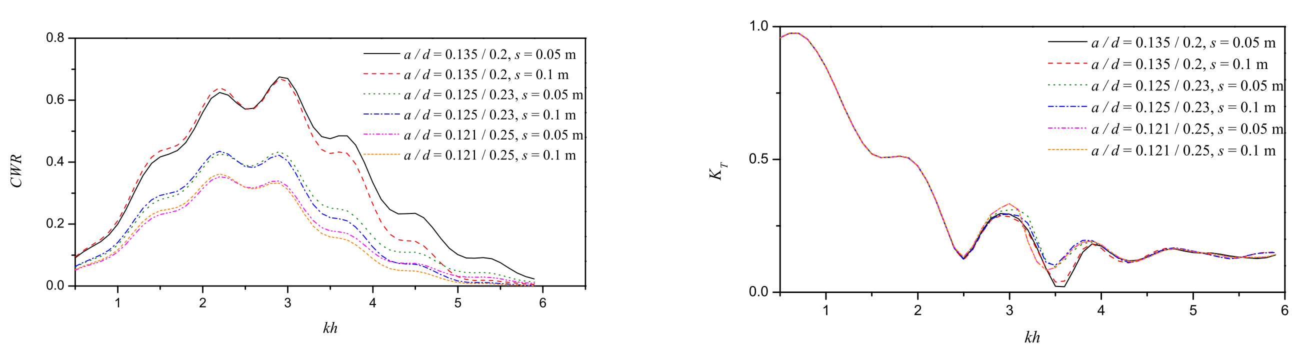

(**a**) (**b**)

Fig. 7 (**a**) CWR and (**b**) K_T as a function of *kh* with different ratios of radius to draft of the cylindrical WEC and different gap widths between the cylindrical WEC and the breakwater.

Fig. 7(a) shows CWR as a function of *kh* with different ratios of radius to draft of the cylindrical WEC and different gap widths between the WEC and the breakwater, *s*. It indicates that CWR is sensitive to the changes in *a/d*. When *a/d* decreases, the CWR reduces significantly. While the different gap widths varying from 0.05 m to 0.1 m have a relatively less significant influence on CWR than the changes in *a/d*. Fig. 7(b) shows K_T as a function of *kh* with different ratios of radius to draft of the cylindrical WEC and different gap widths, it suggests that the ratio of radius to draft and gap width have only a minor influence on K_T.

4.2 Cylinder with fixed arc structure

To optimise the WEC-B, an original idea which uses a fixed arc structure installed around the cylindrical WEC, as shown in Fig. 8, is investigated. The fixed arc structure is designed to re-reflect waves to increase reflected waves on the cylindrical WEC and increase CWR. For practical utilisation, the fixed arc structure can be attached to the rod of the pile restraint for the cylindrical WEC. Meanwhile, the volume of the arc structure in the following parametric research (a_2 equals 0.22 m; d_1 varying from 0.15 m to 0.20 m) is always set to be smaller than half the volume of the cylindrical WEC. The construction cost of the structure is controlled by total volume (i.e., total mass with the same density) in this research. Thus, the installation of this extra setup should be considered much cheaper than the installation of another new cylindrical WEC buoy, and the new setup should not be difficult to implement in practical utilisations. The gap width between the cylindrical WEC and the inner side of the arc structure is 0.05 m (a_1 = a + 0.05 m), which equals the gap width between the cylindrical WEC and the breakwater.

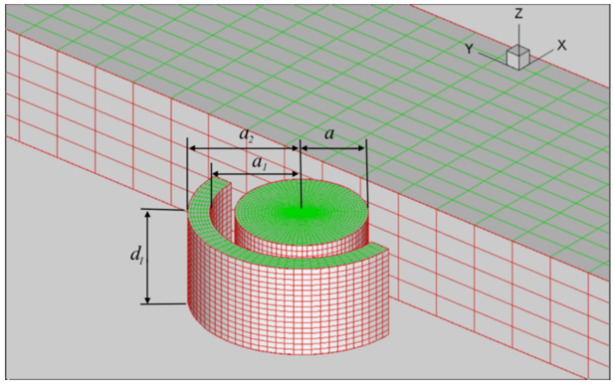

Fig. 8 A new setup with a fixed arc structure installed around the cylindrical WEC (model setup in HAMS®).

4.2.1 Angle of the Arc

Three angles of the arc structure with a_2 of 0.22 m are investigated below and shown in Fig. 9. Fig. 10(a) shows CWR as a function of *kh* with different angles of a fixed arc structure. CWR in Fig. 10(a) increases, especially in the high wave frequency region when a 90° or 180° arc is installed, compared with CWR of the cylindrical WEC without the arc. However, when the arc angle is 270°, CWR reduces and is even lower than the CWR of the cylindrical WEC without the arc. So, based on these comparisons, the 180° arc is the best setup for the cases investigated here, and CWR keeps a high value with a wide range of *kh*. Fig. 10(b) shows K_T as a function of *kh* with different angles of a fixed arc structure. The presence of an arc structure does not obviously influence the performance of the breakwater on KT. In addition, when the best setup with the 180° arc is applied, K_T is at a low value in the high-frequency region, which refers to a good performance on transmitted wave height reduction of the breakwater, the WEC can also keep a good performance on wave energy conversion with a high value of CWR in this wave frequency region.

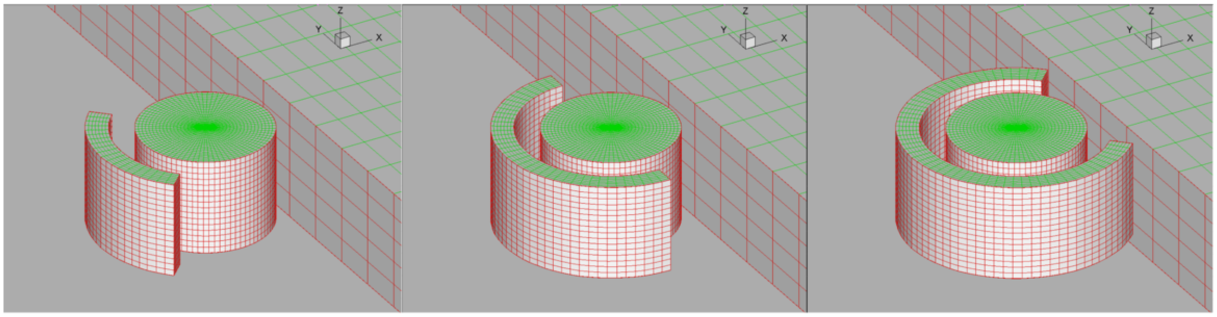

90º Arc 180º Arc 270º Arc

Fig. 9 The fixed arc structure with different angles (model setup in HAMS®).

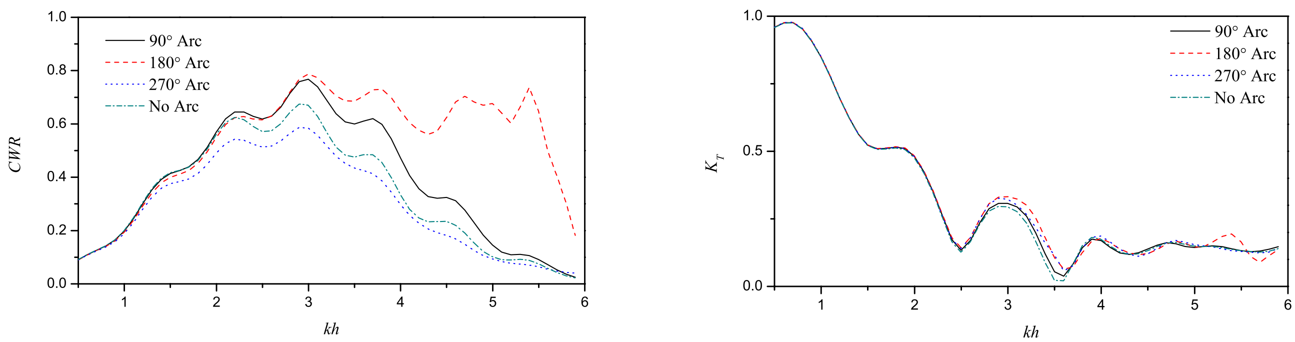

(**a**) (**b**)

Fig. 10 (**a**) CWR and (**b**) K_T as a function of *kh* with different angles of a fixed arc structure.

4.2.2 Draft of the Arc

Fig. 11(a) shows diagrams of CWR with different drafts of the arc (d_1). Compared with the CWR of the cylindrical WEC without arc, an arc structure with all these drafts listed in Fig. 11 can improve the peak value of CWR and keep CWR at a high value in the broader region of *kh*. In addition, the increase of the draft of the arc structure can improve the CWR continuously. K_T as a function of *kh* with a different outer radius of the arc is shown in Fig. 11(b). Identical to the other parameters, the draft has only a minor effect on K_T in Fig. 11(b).

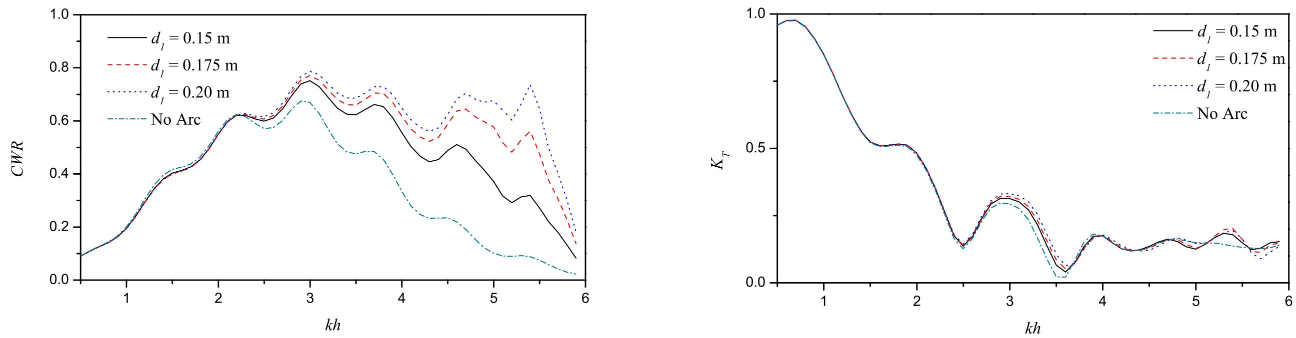

(**a**) (**b**)

Fig. 11 (**a**) CWR and (**b**) K_T as a function of *kh* with different drafts of a fixed arc structure.

4.2.3 Comparison between the modified HAMS® and OpenFOAM®

To check the accuracy of the results obtained from the modified HAMS®, the optimised setup of the cylinder with arc system simulated by OpenFOAM® is compared with the modified HAMS® results. Fig. 12 shows the setup and the visualised simulations when a wave crest passes the WEC-B system in OpenFOAM.

Four test cases, the cylinder without arc with the incident wave period of 1.17 s (*kh* = 2.956) and 0.90 s (*kh* = 4.969), and the cylinder with arc with the incident wave period of 1.17 s (*kh* = 2.956) and 0.90 s (*kh* = 4.969), are simulated by OpenFOAM®. Fig. 13 shows the comparisons between the four points of the four test cases simulated by OpenFOAM® and the curves of HRAO as a function of *kh* predicted by the modified HAMS®. The HRAO simulated by OpenFOAM® presents identical predictions as the modified HAMS® that the cylindrical WEC with arc has a relatively larger heave response than the WEC without arc. Fig. 13 indicates the reliability of the modified HAMS® in this paper to predict the accurate changes of HRAO with the presence of an arc structure. A larger HRAO will increase the CWR of WEC (as the relations in Eq. 4), and the arc structure is supposed to be able to improve the performance of the WEC-B system in practical situations.

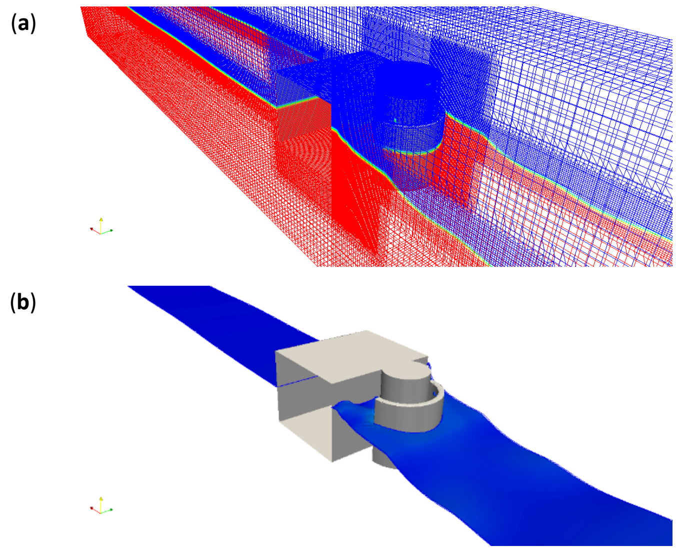

Fig. 12 (a) Mesh and (b) surface snapshot of the visualization for the simulation by OpenFOAM when a wave crest is passing the WEC-B system and cylindrical WEC is in an elevated position.

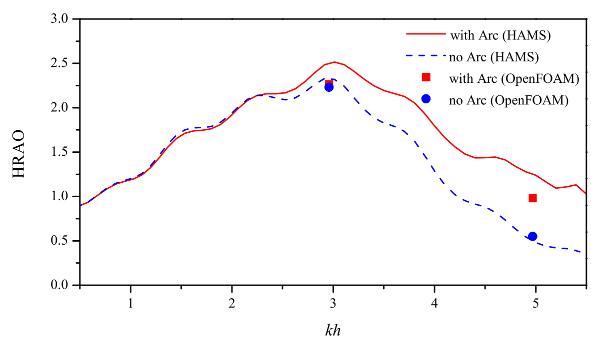

Fig. 13 Comparison of HRAO of cylindrical WEC as a function of *kh* between the modified HAMS results and OpenFOAM results.

5. Conclusions

This paper has employed the CFD model (OpenFOAM®) to modify a potential flow solver (HAMS®) to undertake parametric research to optimise an integrated cylindrical WEC-type breakwater system. Validations have been conducted to confirm the accuracy of this method. Both the variation and magnitude of CWR and K_T of the WEC-B system as a function of *kh* were predicted using an efficient numerical approach. The ratio of radius to draft of the cylindrical WEC was investigated for optimisation. A new setup based on the original concept was proposed to increase the potential efficiency of wave energy extraction of the WEC-breakwater system to about 80% from 70% in [4]. In addition, the performance of wave energy extraction of the concept of heave oscillating WEC without arc structure in the high wave frequency region (dimensionless wave number $kh > 4$) is notably improved with the new concept setup.

ACKNOWLEDGMENT

Computations of CFD models were performed on the HPC facility "Balena" at the University of Bath.

FUNDING

This research was partially funded by the Royal Academy of Engineering (Grant No. UK-CIAPP/73), and the UK EPSRC (Grant No. EP/M022382/1).

REFERENCES

[1] Vicinanza, D., Contestabile, P., Quvang Harck Nørgaard, J., Lykke Andersen, T., 2014, "Innovative rubble mound breakwaters for overtopping wave energy conversion," Coast. Eng., 88 (2014), pp. 154–170. doi:10.1016/j.coastaleng.2014.02.004.

[2] Güney, M.S., Kaygusuz, K., 2010, "Hydrokinetic energy conversion systems: A technology status review. Renew," Sustain. Energy Rev., 14 (2010), pp. 2996–3004. doi:10.1016/j.rser.2010.06.016.

[3] Zhao, X., Ning, D., Zou, Q., Qiao, D., Cai. S., 2019, "Hybrid floating breakwater-wec system: a review," Ocean Eng., 186 (2019), pp. 106-120. doi:10.1016/j.oceaneng.2019.106126.

[4] Zhao, X.L., Ning, D.Z., Liang, D.F., 2019, "Experimental investigation on hydrodynamic performance of a breakwater-integrated WEC system," Ocean Eng., 171 (2019), pp. 25–32. doi:10.1016/j.oceaneng.2018.10.036.

[5] McCabe, A.P., Aggidis, G.A., 2009, "Optimum mean power output of a point-absorber wave energy converter in irregular waves," Proc. Inst. Mech. Eng. Part A J. Power Energy, 223 (2009), pp. 773–781. doi:10.1243/09576509JPE751.

[6] Jin, S., Patton, R., 2017, "Geometry influences on hydrodynamic responses of a heaving point absorber wave energy converter," EWTEC, Southampton, UK.

[7] Jacobsen, N.G., Fuhrman, D.R., Fredsøe, J., 2012, "A wave generation toolbox for the open-source CFD library: OpenFoams," Int. J. Numer. METHODS FLUIDS, 70 (2012), pp. 1073–1088. doi:10.1002/fld.2726.

[8] Liu, Y., 2019, "HAMS: A frequency-domain preprocessor for wave-structure interactions-Theory, development, and application," J. Mar. Sci. Eng., 7 (2019) pp. 1–19. doi:10.3390/jmse7030081.

[9] Liu, Y., Yoshida, S., Hu, C., Sueyoshi, M., Sun, L., Gao, J., Cong, P., He, G., 2018. "A reliable open-source package for performance evaluation of floating renewable energy systems in coastal and offshore regions," Energy Convers. Manag., 174, pp. 516-536, doi: 10.1016/j.enconman.2018.08.012.

[10] Liu, Y., 2021. "Introduction of the Open-Source Boundary Element Method Solver HAMS to the Ocean Renewable Energy Community," Proc. EWTEC 2021, Plymouth, UK.

[11] Lee, H., Poguluri, S.K., Bae, Y.H., 2018, "Performance analysis of multiplewave energy converters placed on a floating platform in the frequency domain," Energies, 11 (2018). doi:10.3390/en11020406.

[12] Ning, D., Zhao, X., Göteman, M., Kang, H., 2016, "Hydrodynamic performance of a pile-restrained WEC-type floating breakwater: An experimental study," Renew. Energy, 95(2016), pp. 531–541. doi:10.1016/j.renene.2016.04.057.

[13] Chen, L.F., Zang, J., Hillis, A.J., Morgan, G.C.J., Plummer, A.R., 2014, "Numerical investigation of wave-structure interaction using OpenFOAM," Ocean Eng, 88 (2014), pp. 91–109. doi:10.1016/j.oceaneng.2014.06.003.

[14] Ding, H., Zang, J., Ning, D., Zhao, X., Chen, Q., Blenkinsopp, C., Gao, J., 2019, "Evaluation of the performance of an integrated wec type of breakwater system," Proc. Int. Conf. Offshore Mech. Arct. Eng. – OMAE, doi:10.1115/OMAE2019-95739.